

Stamp printing of silicon-nanomembrane-based photonic devices onto flexible substrates with a suspended configuration

Xiaochuan Xu,^{1,†,*} Harish Subbaraman,^{2,†} Amir Hosseini,² Che-Yun Lin,¹ David Kwong,¹ and Ray T. Chen^{1,3}

¹Microelectronics Research Center, The University of Texas at Austin, Austin, Texas 78758, USA

²Omega Optics, Incorporated, 10306 Sausalito Drive, Austin, Texas 78759, USA

³e-mail: raychen@uts.cc.utexas.edu

*Corresponding author: xiaochuan.xu@mail.utexas.edu

Received September 28, 2011; revised January 2, 2012; accepted January 5, 2012;
posted January 9, 2012 (Doc. ID 155424); published March 8, 2012

In this Letter, we demonstrate for the first time (to our best knowledge) stamp printing of silicon nanomembrane (SiNM)-based in-plane photonic devices onto a flexible substrate using a modified transfer printing method that utilizes a suspended configuration, which can adjust the adhesion between the released SiNM and the “handle” silicon wafer. With this method, 230 nm thick, 30 μm wide, and up to 5.7 cm long SiNM-based waveguides are transferred to flexible Kapton films with >90% transfer yield. The propagation loss of the transferred waveguides is measured to be ~ 1.1 dB/cm. Scalability of this approach to transfer intricate structures, such as photonic crystal waveguides and multimode interference couplers with a minimum feature size of 200 nm and 2 μm , respectively, is also demonstrated. © 2012 Optical Society of America

OCIS codes: 220.4000, 220.4241, 130.1750, 130.5296.

To date, most flexible electronics/phonics rely on organic, polymer and amorphous semiconductor material systems. One significant advantage of such materials is that the devices can be fabricated directly onto flexible substrates with conventional low-temperature processes such as ink-jet printing, screen printing, and molding. However, the device performance achievable is still inferior compared with single-crystal-semiconductor-based devices. Since the discovery that thin single crystal films can also possess extreme flexibility yet retain bulk material properties [1,2], new opportunities in flexible electronics and phonics have been explored. Among all transferable single-crystal semiconductors, the silicon nanomembrane (SiNM) is one of the most promising materials because it possesses not only high carrier mobility and mechanical durability, but also optical transparency in the near-IR region, thus making it suitable for high-performance flexible optoelectronic devices. In the conventional SiNM transfer method, the patterned silicon-on-insulator (SOI) chip is put into hydrofluoric (HF) solution to selectively remove the buried oxide (BOX) layer [1–11]. The released SiNM settles down and is weakly bonded to the “handle” silicon wafer via van der Waals forces. For the above process to work, the thickness of the BOX must be less than 500 nm in order to prevent shifting of devices during the settling process [3]. However, if the BOX is too thin, the time required for its complete undercut etching is prohibitively long because the edges of the SiNM settle down to the handle silicon and block HF penetration. A BOX thickness of 150–200 nm has been found to be optimum for the transfer process [3–5]. Upon complete undercutting of the BOX, the SiNM is peeled up and transfer printed onto other foreign substrates with the help of an elastomeric stamp. The adhesion between the stamp and the SiNM can be kinetically controlled by adjusting the peel-

ing speed [4]. Through this approach, important progresses have been made in flexible electronics and surface normal photonics, including flexible and rollable paperlike displays [6], flexible silicon integrated circuits [5], nanostructure Fano filters [7], and smart skins [8]. In contrast to the rapid progress in SiNM-based electronics, very little progress has been reported for in-plane flexible photonics because the optical properties of in-plane flexible photonic devices are very geometrically dependent and hence greatly affected by shifts, wrinkles, and cracks that are frequently observed within the conventional stamp printing process. A potential alternative is to bond the SOI upside down onto the target substrate and then remove the handle silicon by polishing or deep silicon etching [9]. However, this process is not very economically viable because the handle wafer is entirely destroyed.

In our previous work, we demonstrated the possibility of transferring photonic crystal waveguides (PCWs) and multimode interference (MMI) couplers onto flexible polyimide substrate through the conventional direct-peeling-up approach [10]. Without an elastomeric stamp, adhesion between the surfaces is difficult to control, resulting in a low transfer yield. Besides, possibly due to the formation of the $-\text{Si}-\text{O}-\text{Si}-$ bonds between the released SiNM and the handle silicon [11], in some cases, it is very difficult to pick the SiNM up after undercut etching, even with highly adhesive surfaces, for example, Scotch tape. Furthermore, for a complicated structure, the undercut etching time of different regions is unequal. Therefore, some parts of the SiNM are fully free, while other areas are still held by the BOX, causing shifts or even cracks. In this Letter, we present a stamp printing method exploiting supporting layer and adjustable pedestals, with which 30 μm wide, 230 nm thick, up to 5.7 cm long multimode waveguides are transferred onto a

flexible substrate with yield >90%. The propagation loss of the transferred waveguide is measured to be ~ 1.1 dB/cm, which is comparable with waveguides on SOI. This method has also been applied to transfer other intricate structures, such as PCW and MMI, with minimum feature sizes of 200 nm and 2 μm , respectively, and this process is relatively independent of the thickness of the BOX. According to the authors' best knowledge, this is the first demonstration of operational SiNM-based in-plane flexible photonic devices, which we believe could open an entirely new field with a wide range of useful applications.

A 30 μm wide, 8 mm long waveguide is fabricated with commercially available SOI from Soitec with 250 nm single crystal silicon, 3 μm BOX, and 500 μm handle silicon. The SOI is first oxidized to create a 45 nm oxide layer as a hard mask for silicon etching, leaving a silicon layer of 230 nm. After electron beam lithography (JEOL JBX-6000), a 20 nm nickel layer is deposited and a standard lift-off process is used to invert the pattern. The pattern is transferred to the silicon oxide hard mask by reactive ion etching (RIE). The metallic layer is then removed by piranha cleaning. A HBr/Cl_2 RIE etch is used to transfer the pattern to the silicon layer, as shown in Fig. 1(a).

To form pedestals, the patterned sample is put into a 6:1 buffered oxide etch (BOE) for 5 min to partially remove the silicon dioxide underneath the waveguide, as shown in Fig. 1(b). Then, ~ 1.7 μm AZ 5214 photoresist is spin coated (4000 rpm, 30 s). The resist also fills the exposed edges under the waveguides, thus forming polymeric pedestals, as shown in Fig. 1(c). An array of holes with diameter of 100 μm and pitch of 200 μm is patterned on the resist to let the etchant penetrate for BOX removal. The sample is hard baked at 110 $^\circ\text{C}$ for 3 min, and then put into a beaker filled with HF vapor. The HF vapor can be generated simply by covering a beaker with concentrated HF solution. The etch rate is ~ 50 $\mu\text{m}/\text{h}$, which can be controlled by opening different sizes of holes on the cover. After completely removing the BOX, the SiNM, protected by the photoresist, will settle down to the handle silicon. The supporting layer and vapor etching sufficiently prevent the SiNM from the shifting caused by the fluid flows. The result can be further improved by heat-

ing the sample up to let the by-product water from the chemical reaction evaporate. After gently cleaning and drying the sample with nitrogen, oxygen plasma is used to remove the photoresist everywhere, except the region underneath the SiNM, as shown in Fig. 1(d). The center region of the SiNM sags down and contacts the underlying substrate. The contact area can be controlled by tuning the dimensions of the pedestal through adjusting the first step BOX etching time. This controllability is important because when the contact area becomes too large, it becomes very difficult to peel the SiNM up. The etching time is controlled in order to initiate sufficient delamination between the SiNM and silicon surface during retrieval with an elastomeric stamp. In this Letter, the etching time is optimized to 5 min, forming a pedestal ~ 200 nm high.

A polydimethylsiloxane (PDMS) stamp is prepared by mixing the base and agent with a ratio of 6:1, and then they are cured at 90 $^\circ\text{C}$ for 2 h. The stamp is bonded to a glass slide through activating both surfaces with oxygen plasma and 2 h 90 $^\circ\text{C}$ annealing. Bringing the stamp into contact with the substrate and then peeling it back at high speed lifts the SiNM structure from the handle silicon, as shown in Fig. 1(e) [4,5]. A 125 μm thick polyimide film (Kapton, DuPont) is cleaned with acetone and methanol. ~ 7 μm thick NOA 61 (Norland Optical Adhesive) is spin coated (4000 rpm, 60 s). The epoxy is precured for 10 min (7.5 mW/cm^2). Then, the "inked stamp" is brought into contact with the precured epoxy film. The film is fully cured from the top side down through the PDMS, and the stamp is slowly retrieved, leaving the SiNM on the flexible substrate, as shown in Fig. 1(f). The whole sample is put into an oven at 60 $^\circ\text{C}$ for 12 h to achieve better adhesion between the NOA 61 and SiNM. The fully cured NOA 61 has good transmission at 1550 nm with a refractive index of ~ 1.54 . The scanning electron microscope (SEM) and the optical microscope images for the corresponding steps outlined in Fig. 1 are shown in Fig. 2. More than 420 waveguides (30 chips) are transferred, and more than 380 of them are successful, indicating a yield of >90%.

In order to test the transferred waveguides, the end facets are prepared. The flexibility of the SiNM, NOA 61, and Kapton makes it very difficult to prepare the end facets of the SiNM waveguide for light coupling. Therefore, we first use RIE (CHF_3/O_2) to etch the end of the waveguide and the NOA 61 underneath away. Then, the Kapton substrate is diced less than 14.5 μm away from the edge of the waveguide in order to enable light coupling using a polarization maintaining lensed fiber with a working distance of 14.5 μm and spot diameter of 2.5 μm . The cross section of the prepared facet is shown in Fig. 3(a). The output light from the waveguide is collected with a multimode fiber with a mode diameter of 50 μm . The sample is taped down to a glass slide. Through a top-down IR camera, as shown in Fig. 3(b), the output spot can be clearly observed, indicating strong light emission. The measured insertion loss is ~ 25 dB for the 7 mm transferred waveguide, which is about 6 dB more than the waveguide before transfer, as shown in Fig. 3(c). This is possibly due to the increase of facet roughness caused by the mechanical vibration during the dicing process. To measure the propagation loss of the waveguide,

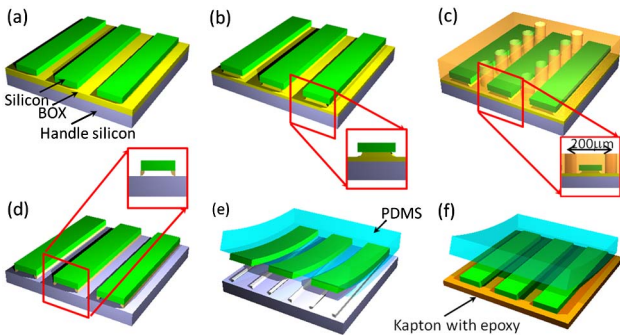


Fig. 1. (Color online) Schematic illustration of the stamp printing process exploiting a suspension structure. (a) Patterned SOI chip. (b) Illustration of chip after first undercut etching. (c) Application and patterning of the supporting layer. (d) SiNM suspension on pedestals after complete undercut etching. (e) Peeling up of the released SiNM with PDMS stamp. (f) Printing of SiNM devices onto a polyimide film.

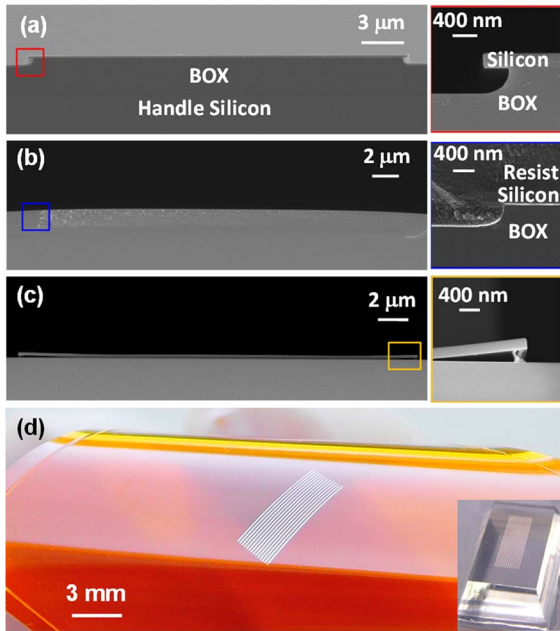


Fig. 2. (Color online) (a)–(c) SEM image of the cross section of the SiNM. (a) After BOE etching for 5 min. (b) After spin casting the photoresist. (c) After full undercut etching and removing the photoresist with oxygen plasma. (d) Transferred SiNM waveguide showing good flexibility and the PDMS “inked” with SiNM (inset).

a structure shown in Fig. 3(d) is transferred. Through varying ΔL , the length of the waveguide can be changed by 2.6 cm. The measured loss is ~ 1.1 dB/cm in the region from 1530 to 1600 nm, which is comparable with the SOI-based waveguide. This transfer technique has been used to also transfer intricate devices such as 1×6 MMI and PCW, with a minimum dimension of $2 \mu\text{m}$ and 200 nm , as shown in Figs. 4(a) and 4(b), respectively, which are not feasible to be transferred using the conventional

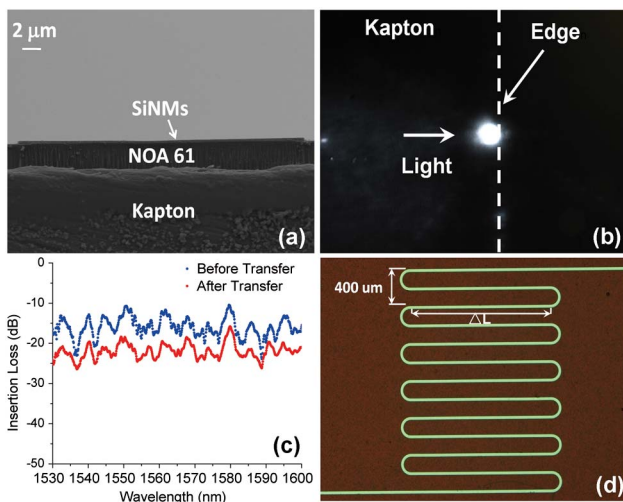


Fig. 3. (Color online) (a) SEM image of the cross section of the waveguide after transfer. (b) Output spot captured by an top-side-down IR camera. (c) Insertion loss of 7 mm SiNM-based flexible waveguide (red lower curve) and the SOI-based waveguide (blue upper curve) (d) Structure used to measure the propagation loss of the waveguide.

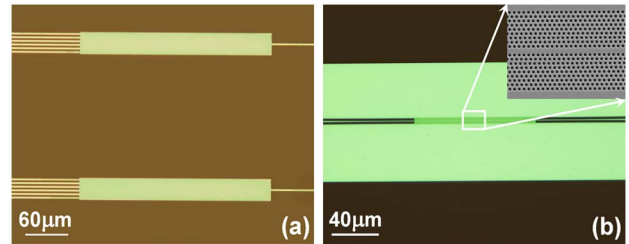


Fig. 4. (Color online) (a) Transferred 1×6 MMI couplers. (b) Transferred PCW.

approach. Further results of these nanophotonic devices will be presented in future publications.

In summary, we have developed a new stamp printing process based on the supporting layer and suspension structure. With this method, a SiNM-based waveguide up to 5.7 cm long is transferred to flexible substrate, and the measured propagation loss is found to be ~ 1.1 dB/cm. Intricate SiNM devices such as MMI and PCW, which are difficult to transfer using the conventional techniques, have also been transferred successfully using our technique. This demonstration opens vast possibilities for a whole new area of high-performance flexible photonic components using SiNM technology.

The authors acknowledge Prof. John A. Rogers of the University of Illinois at Urbana–Champaign for sharing the experience of the stamp printing process. This research was funded by the Air Force Office of Scientific Research (AFOSR) Multidisciplinary University Research Initiative (MURI) grant (grant no. FA 9550-08-1-0394) and Small Business Innovative Research (grant no. FA 9550-11-C-0014) monitored by Dr. Gernot Pomrenke.

[†]These authors contributed equally to this work.

References

1. F. Cavallo and M. G. Lagally, *Soft Matter* **6**, 439 (2010).
2. J. A. Rogers, M. G. Lagally, and R. G. Nuzzo, *Nature* **477**, 45 (2011).
3. G. X. Qin, H. C. Yuan, G. K. Celler, W. D. Zhou, and Z. Q. Ma, *J. Phys. D* **42**, 234006 (2009).
4. M. A. Meitl, Z. T. Zhu, V. Kumar, K. J. Lee, X. Feng, Y. Y. Huang, I. Adesida, R. G. Nuzzo, and J. A. Rogers, *Nat. Mater.* **5**, 33 (2005).
5. D. H. Kim, J. H. Ahn, W. M. Choi, H. S. Kim, T. H. Kim, J. Z. Song, Y. G. Y. Huang, Z. J. Liu, C. Lu, and J. A. Rogers, *Science* **320**, 507 (2008).
6. J. A. Rogers, Z. Bao, K. Baldwin, A. Dodabalapur, B. Crone, V. R. Raju, V. Kuck, H. Katz, K. Amundson, J. Ewing, and P. Drzaic, *Proc. Natl. Acad. Sci. USA* **98**, 4835 (2001).
7. W. D. Zhou, Z. Q. Ma, H. J. Yang, Z. X. Qiang, G. X. Qin, H. Q. Pang, L. Chen, W. Q. Yang, S. Chuwongin, and D. Y. Zhao, *J. Phys. D* **42**, 234007 (2009).
8. T. Someya, Y. Kato, S. Iba, Y. Noguchi, T. Sekitani, H. Kawaguchi, and T. Sakurai, *IEEE Trans. Electron. Dev.* **52**, 2502 (2005).
9. M. J. Zablocki, A. Sharkawy, O. Ebil, and D. W. Prather, *Opt. Lett.* **36**, 58 (2011).
10. A. Ghaffari, A. Hosseini, X. C. Xu, D. Kwong, H. Subbaraman, and R. T. Chen, *Opt. Express* **18**, 20086 (2010).
11. Y. Yang, Y. Hwang, H. A. Cho, J. H. Song, S. J. Park, J. A. Rogers, and H. C. Ko, *Small* **7**, 484 (2011).